Available online at www.sciencedirect.com

SciVerse ScienceDirect

Energy Procedia 37 (2013) 4698 – 4711

Energy Procedia

GHGT-11

Safety-Based Injection Strategy for Carbon Dioxide Geological Sequestration in a Deep Saline Aquifer with Complex Sandstone-Shale Sequences: A Case Study from Taiwan

Bieng-Zih Hsieh[a,]*, Cheng-Yueh Wu[a], Chi-Chung Tseng[a,b], Ta-Lin Chen[b], Zsay-Shing Lin[a]

[a]*Department of Resources Engineering, National Cheng Kung University, 1 University Road, Tainan 701, Taiwan*
[b]*Exploration and Development Research Institute, CPC Corporation, Taiwan, 1 Ta Yuan, Wen Fa Road, Miaoli 360, Taiwan*

Abstract

The purpose of this study was to decide the best injection strategy for CO_2 geo-sequestration in a deep saline aquifer with complex bedded sandstone-shale sequences. The best injection strategy is decided based on the estimates of the safety index (SFI). Numerical simulation method was used in this study. The major conclusions from this study are: (1) Safe trapping mechanisms contribute to a lower risk of CO_2 leakage by trapping CO_2 as immobile blobs or changing the phase of CO_2 from supercritical phase to aqueous, ionic, and mineral phases in the post-injection period. (2) For an aquifer with complex sandstone-shale sequences, the best injection strategy should be decided by the results of risk evaluation and the SFI estimation. (3) The well location affected the injection strategy. The risk of CO_2 leakage was lower using a down-dip injection well than an up-dip well. (4) The best strategy for this case study was to use the down-dip well to inject CO_2 into the bottom sandstone layer. The SFI for this scenario reached 0.99 at the storage time of 1000 years, which meant that the probability of CO_2 leakage occurring was nearly zero.

Keywords: CO_2 sequestration; Deep saline aquifer; Numerical Simulation; Safety Index; Trapping Mechanism

1. Introduction

Carbon dioxide (CO_2) capture and storage (CCS) is a feasible technique of effectively reducing greenhouse gas emissions to the atmosphere. The purpose of CCS technology is to capture CO_2 produced from an industrial activity, and to store it safely and permanently in an appropriate storage site. CO_2 storage methods include geological sequestration, ocean storage, and mineral carbonation. The most feasible method for storing CO_2 is geological sequestration [1].

1876-6102 © 2013 The Authors. Published by Elsevier Ltd.
Selection and/or peer-review under responsibility of GHGT
doi:10.1016/j.egypro.2013.06.379

The major types of CO_2 geological sequestration (or geo-sequestration) include depleted oil and gas reservoirs, deep saline aquifers, and coal seams [2]. Depleted oil and gas reservoirs are suitable sites for CO_2 geo-sequestration because they have already proved able to hold and safely store gas for spans of geologic timescales [3]. However, deep saline aquifers have the greatest storage potential of all the geological options, and can be found in most of the sedimentary basins that are close to the emission sources [4].

Injection efficiency and storage safety are the essential considerations when CO_2 is stored in any geological structure or a CO_2 geo-sequestration project on any scale is implemented. Injection efficiency should consider the problem of rock failure while CO_2 is being injected into a formation. In addition, the injected CO_2 should be permanently stored in a formation without any leakage. In other words, the risk of stored CO_2 leakage should as low as possible.

The issue of storage safety is more significant in a deep saline-aquifer geo-sequestration because it is unlike a depleted gas reservoir for which the cap rock integrity has proved to have the potential to store CO_2 permanently.

The safety-based injection strategy introduced in this study is an engineering strategy for considering not only the injection efficiency for injecting million of tons of CO_2 per year, but also the safety demand for reaching the lowest risk of CO_2 leakage when it is stored in a deep saline aquifer. By investigating the contributions of the safe trapping mechanisms—residual gas, solubility, ionic, and mineral trappings—the risk of CO_2 leakage can be estimated, and then the best safety-based injection strategy can be decided.

The purpose of this study was to decide, for a demonstration CO_2 geo-sequestration project in Taiwan, the best safety-based injection strategy for CO_2 geological sequestration in a deep saline aquifer with complex bedded sandstone-shale sequences.

2. Safety index used for the best injection strategy decision

CO_2 can be trapped in a saline aquifer by five mechanisms: structural, residual gas, solubility, ionic, and mineral trapping mechanisms. The CO_2 trapped by structural trapping is a form of mobile gas (or supercritical) phase. Residual gas, solubility, ionic, and mineral trappings are relatively safe and low-risk trapping mechanisms [5]. The greater the percentage of CO_2 trapped by the safe trapping mechanisms, the safer the CO_2 sequestration.

The safety index (SFI) used in this study to evaluate the risk of CO_2 leakage and then to decide the best injection strategy was defined as follows [5]:

$$SFI = (n_{CO2(res)} + n_{CO2(aq)} + n_{CO2(ion)} + n_{CO2(min)})/n_{CO2(inj)} \tag{1}$$

where **SFI** is the safety index; $\mathbf{n_{CO2(res)}}$ is the number of moles of the immobile supercritical phase CO_2, which was calculated from the residual gas saturation of CO_2; $\mathbf{n_{CO2(aq)}}$ is the number of moles of the aqueous phase CO_2, which was calculated from the mole fraction of CO_2 in the aqueous phase; $\mathbf{n_{CO2(ion)}}$ is the moles of the ionic phase CO_2, which was estimated from the concentration (or molality) of bicarbonate and carbonate ions in the chemical equilibrium reactions; $\mathbf{n_{CO2(min)}}$ is the number of moles of the mineral phase CO_2, which was estimated from the changes in the number of moles of minerals in the geochemical mineral reactions; and $\mathbf{n_{CO2(inj)}}$ is the cumulative number of moles of injected CO_2 at the current time, which were calculated from the injection rate and the injection time.

The number of moles of CO_2 trapped by the trapping mechanisms, which is used to estimate the SFI, is dynamic and changes with time after CO_2 has been injected into a deep saline aquifer.

3. Geological Description

The storage reservoir used for this case study was the Y-sandstone formation located in the T-field in northwestern Taiwan (Fig. 1), which is a deep saline aquifer with complex sandstone-shale sequences.

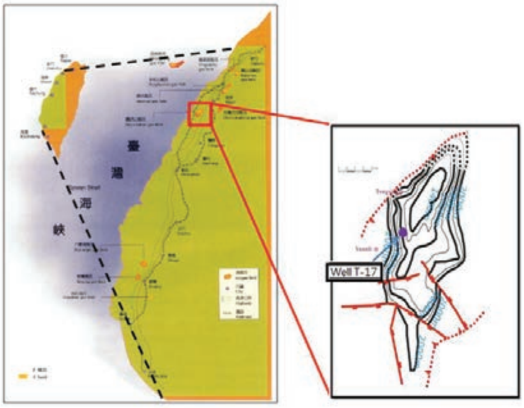

Fig. 1. (a) Location of the target storage reservoir; (b) Structure map of the Y-sandstone formation

The Y-sandstone formation is one of the members of the K-formation (Fig. 2). The K-formation is divided into three members: Y-sandstone, L-shale, and T-sandstone (Fig. 2). The Y-sandstone is the top layer of the K-formation and is overlaid by the impermeable C-shale formation. The C-shale formation is approximately 300 meters thick, and its permeability is extremely low. The C-shale formation is considered an excellent cap rock that will prevent CO_2 leakage after CO_2 has been injected into the Y-sandstone for storage. Beneath the Y-sandstone is the L-shale, which is treated as the impermeable lower boundary of the CO_2 storage formation (i.e., the Y-sandstone) to help provide the injected CO_2 with safe storage (Fig. 2).

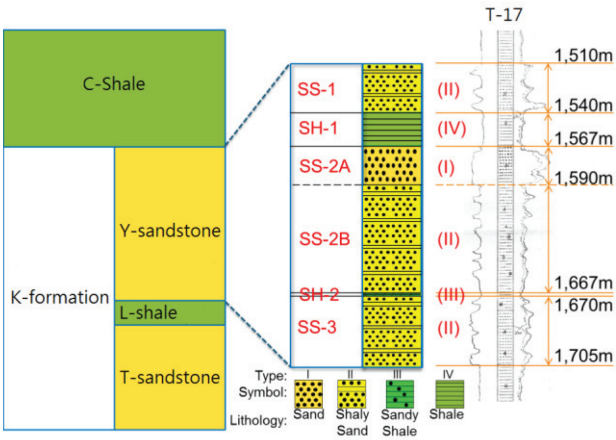

Fig. 2. (a) Formation sequences of the storage site; (b) Lithology of the major layers in the Y-sandstone formation

The Y-sandstone is a sandstone-shale sequence formation. From the analysis of geophysical well-logging, five major layers were defined in the Y-sandstone formation, from top to bottom: SS-1 (the top sandstone layer), SH-1 (the first shale layer), SS-2 (the middle sandstone layer), SH-2 (the second shale layer), and SS-3 (the bottom sandstone layer). The SS-2 layer was subdivided to SS-2A (the upper section of SS-2) and SS-2B (the lower section of SS-2) based on its different lithologies. The lithology of the layers of SS-1, SS-2B, and SS-3 are shaly sandstone; SS-2A is sandstone (Fig. 2).

4. Reservoir Simulation Model Construction

The numerical simulation method was used in this study to estimate the SFI from the amount of CO_2 of the different trapping mechanisms when CO_2 was sequestered in the Y-sandstone formation. The GEM compositional simulator with the GEM-GHG module, which is capable of modelling all trapping mechanisms, was used [6-9].

The first step in constructing the reservoir simulation model is digitizing the structure map (Fig. 3). The numerical geological model was developed by dividing the structure into grids using the digitized structure map. The formation parameters of Y-sandstone used in the simulation model were collected from CPC, Taiwan (Table 1).

The rock and fluid properties and the formation's initial conditions (initial formation pressure, reservoir temperature, formation water analysis data, and rock mineral compositions) were assigned to each grid block, and then the operation (injection rates and pressures) and completion (perforation intervals) conditions were designed (Fig. 3). This case study was simulated to inject one million tons of CO_2 per year for 20 years, with the constraint of a monitored injection pressure that had to be lower than the fracture pressure. All the trapping mechanisms (structure, residual gas, solubility, ionic, and mineral trappings) were considered in the simulation model. The total simulation period was 1000 years.

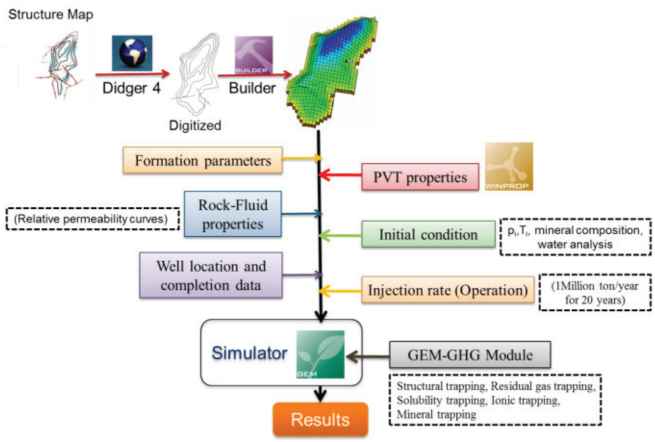

Fig. 3. Flow chart of the numerical simulation model construction

5. Results

Six injection scenarios were designed for the case study of the safety-based injection strategy. Each scenario had a specific well location (located at the up-dip or down-dip of the anticline structure) and perforation interval (perforated in the sandstone layers SS-1, SS-2, or SS-3). Contributions to the quantity of CO_2 trapped by the different trapping mechanisms were estimated. The SFIs of six scenarios were calculated, and the best engineering strategy for this case study was determined.

The injection scenarios (Fig. 4) were designed for: (1) a down-dip well with CO_2 injected into the bottom sandstone layer (SS-3); (2) an up-dip well with CO_2 injected into the bottom sandstone layer (SS-3); (3) a down-dip well with CO_2 injected into the lower section of the middle sandstone layer (SS-2); (4) an up-dip well with CO_2 injected into the lower section of the middle sandstone layer (SS-2); (5) a down-dip well with CO_2 injected into the top sandstone layer (SS-1); and (6) an up-dip well with CO_2 injected into the top sandstone layer (SS-1).

Table 1. Basic rock and fluid parameters of Y-sandstone

Rock and fluid parameters			
Parameter		Value (field unit)	Value (SI unit)
Formation Top		4,265 (ft)	1,300 (m)
Thickness	Gross	672 (ft)	205 (m)
	Sand Interval	539 (ft)	165 (m)
Porosity	Sand	0.2	0.2
	Shaly Sand	0.15	0.15
	Sandy Shale	0.05	0.05
	Shale	0.025	0.025
Permeability	Sand	300 (mD)	$3.06 \times 10^{-13}(m^2)$
	Shaly Sand	225 (mD)	$2.29 \times 10^{-13}(m^2)$
	Sandy Shale	0.001 (mD)	$1.02 \times 10^{-18}(m^2)$
	Shale	1×10^{-9} (mD)	$1.02 \times 10^{-24}(m^2)$
Initial Pressure		2445 (psi) @ 5400 (ft)	16.8 (MPa) @ 1646 (m)
Temperature		162(°F)	72(°C)
Irreducible Water Saturation		0.2	0.2
Salinity		16‰ (16000 ppm)	16‰ (16000 ppm)

Abbreviations: ft, feet; m, meters; mD, millidarcy; psi, pounds per square inch; MPa, megapascals; ppm, parts per million

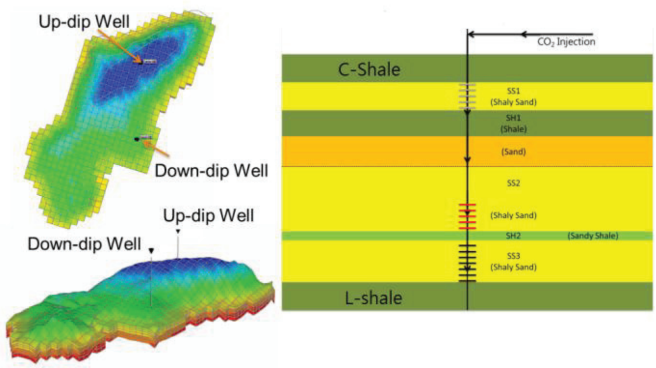

Fig. 4. Well locations and perforated intervals for six injection scenarios

5.1 Down-Dip Well with Bottom Sandstone Layer (SS-3) Injection

In the scenario in which the injection well was located at the down-dip and CO_2 was injected into the bottom sandstone layer (SS-3), 80.11% of a total of 20×10^6 tons of injected CO_2 was stored by structural trapping, and 0.55%, 18.73%, and 0.57% by residual gas trapping, solubility trapping, and ionic trapping, respectively, at the cessation of CO_2 injection (Table 2). Almost no $CaCO_3$ precipitated during CO_2 injection. The percentage of CO_2 trapped by the mineral trapping was less than 0.05% at the end of the injection period (20 years).

The injection of CO_2 was stopped after 20 years. At the end of the simulation (980 years from the cessation of CO_2 injection), the percentages of CO_2 that were trapped by the different trapping mechanisms were 0.01% by structural trapping, 52.73% by residual gas trapping, 24.79% by solubility trapping, 1.14% by ionic trapping, and 21.34% by mineral trapping (Table 2).

Table 2 Contributions of different trapping mechanisms changing with time for scenario (1)

Time (Year)	STM[a] (%)	RTM[b] (%)	SOTM[c] (%)	ITM[d] (%)	MTM[e] (%)
1	71.32	0.00	28.60	0.10	0.00
10	80.04	0.00	19.68	0.28	0.00
15	81.42	0.00	18.07	0.49	0.02
20	80.11	0.55	18.73	0.57	0.04
50	11.88	59.60	26.60	1.14	0.78
70	7.26	62.85	27.26	1.17	1.48
100	4.59	64.16	27.58	1.18	2.49
300	1.05	62.41	26.86	1.17	8.51
500	0.34	59.26	26.05	1.15	13.20
700	0.12	56.42	25.36	1.14	16.97
1000	0.01	52.73	24.79	1.14	21.34

[a]STM: CO_2 trapped by the structural trapping mechanism; [b]RTM: Trapped by residual gas trapping mechanism; [c]SOTM: Trapped by solubility trapping mechanism; [d]ITM: Trapped by ionic trapping mechanism; [e]MTM: Trapped by mineral trapping mechanism.

The percentage of CO_2 trapped by residual gas trapping was markedly low during CO_2 injection because of the drainage process. During the post-injection period, the imbibition process worked behind the migrating plume, and the percentage of CO_2 trapped by residual gas trapping markedly increased (Fig. 5).

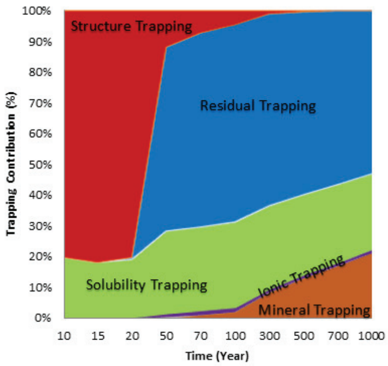

Fig. 5. Diagram of different trapping mechanisms' contributions for scenario (1)

The percentage of CO_2 trapped by solubility trapping was the second highest throughout the duration of CO_2 injection (Fig. 5). The trend of the percentage of CO_2 trapped by ionic trapping was similar to that of solubility trapping in the post-injection period. The percentage of CO_2 trapped by mineral trapping reached 21.34% at the simulation time of 1000 years in the post-injection period (Fig. 5; Table 2).

The percentage of CO_2 trapped by structural trapping (that is, the percentage of mobile supercritical phase CO_2) was markedly high during the CO_2 injection period (Fig. 5). However, it decreased dramatically during the post-injection period because of the formation of residual CO_2 (immobile CO_2).

The SFI for the scenario of the down-dip well with the bottom sandstone layer (SS-3) injection was 0.99 at the storage time of 1000 years.

5.2 Up-dip well with the bottom sandstone layer (SS-3) injection

For the scenario in which the injection well was located at the up-dip and CO_2 was injected into the bottom sandstone layer (SS-3), 82.14% of the total 20 million tons of injected CO_2 was stored by structural trapping, 0.30% by residual gas trapping, 16.88% by solubility trapping, and 0.59% by ionic trapping at the end of the injection period (Table 3). Almost no $CaCO_3$ precipitated during CO_2 injection.

At the end of the simulation, the percentages of CO_2 trapped by the various trapping mechanisms were 9.46% by structural trapping, 42.96% by residual gas trapping, 22.66% by solubility trapping, 1.10% by ionic trapping, and 23.86% by mineral trapping (Table 3).

Table 3 Contributions of different trapping mechanisms changing with time for scenario (2)

Time (Year)	STM (%)	RTM (%)	SOTM (%)	ITM (%)	MTM (%)
1	69.84	0.00	30.07	0.10	0.00
10	79.19	0.00	20.50	0.31	0.01
15	82.85	0.00	16.59	0.50	0.06
20	82.14	0.30	16.88	0.59	0.10
50	40.77	32.32	24.90	1.10	0.94
70	31.56	39.35	26.30	1.18	1.65
100	25.18	44.29	26.61	1.21	2.75
300	14.92	48.82	25.97	1.18	9.14
500	12.82	46.90	24.91	1.16	14.25
700	11.12	45.48	23.74	1.13	18.56
1000	9.46	42.96	22.66	1.10	23.86

Abbreviations: See notes to Table 2.

The percentage of CO_2 trapped by residual gas trapping increased from 0.30% at the end of the injection period (20 years) to 48.82% at the simulation time of 300 years because of the imbibition process (Fig. 6; Table 3). It slightly decreased to 42.96% at 1000 years because the immobile residual CO_2 dissolved in the water in the post-injection period. The percentage of CO_2 trapped by solubility trapping was the second highest throughout CO_2 injection (Fig. 6). The percentage of CO_2 trapped by mineral trapping reached 23.86% at the simulation time of 1000 years in the post-injection period (Fig. 6; Table 3).

The percentage of CO_2 trapped by structural trapping (that is, the percentage of mobile supercritical phase CO_2) was very high (82.14%) during CO_2 injection (Fig. 6; Table 3). It declined during the post-injection period because of the formation of some immobile residual CO_2.

The SFI for the scenario of the up-dip well with the bottom sandstone layer (SS-3) injection was 0.91 at the storage time of 1000 years.

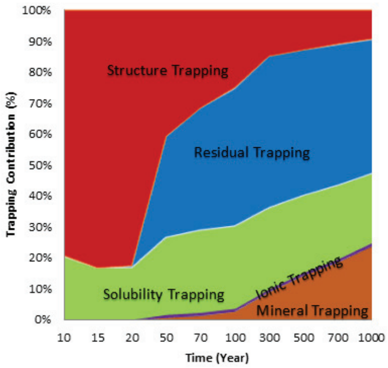

Fig. 6. Diagram of different trapping mechanisms' contributions for scenario (2)

5.3 Down-dip Well with the Lower Section of Middle Sandstone Layer (SS-2) Injection

For the scenario in which the injection well was located at the down-dip and CO_2 was injected into the lower section of the middle sandstone layer (SS-2), 78.91% of injected CO_2 was stored by structural trapping, 4.59% by residual gas trapping, 15.82% by solubility trapping, 0.49% by ionic trapping, and 0.19% by mineral trapping at the cessation of CO_2 injection (20 years) (Table 4).

At the 980 years from the cessation of CO_2 injection, the percentages of CO_2 that were trapped by the different trapping mechanisms were 20.81% by structural trapping, 31.50% by residual gas trapping, 22.03% by solubility trapping, 1.07% by ionic trapping, and 24.58% by mineral trapping (Table 4).

Table 4 Contributions of different trapping mechanisms changing with time for scenario (3)

Time (Year)	STM (%)	RTM (%)	SOTM (%)	ITM (%)	MTM (%)
1	67.11	1.94	30.85	0.11	0.00
10	81.63	0.00	18.06	0.29	0.03
15	79.77	3.25	16.42	0.42	0.13
20	78.91	4.59	15.82	0.49	0.19
50	32.22	46.06	19.44	0.97	1.31
70	29.60	47.84	19.43	0.97	2.15
100	27.48	48.98	19.22	0.96	3.37
300	25.17	46.20	18.04	0.86	9.73
500	23.84	42.17	18.55	0.89	14.55
700	22.58	37.88	19.74	0.95	18.86
1000	20.81	31.50	22.03	1.07	24.58

Abbreviations: See notes to Table 2.

The percentage of CO_2 trapped by residual gas trapping was markedly low during CO_2 injection. However, it was the highest during the post-injection period (Fig. 7). The percentage of CO_2 trapped by solubility trapping was the second highest throughout CO_2 injection (Fig. 7). The percentage of CO_2 trapped by mineral trapping reached about 25% at the simulation time of 1000 years in the post-injection period (Fig. 7; Table 4).

The percentage of CO_2 trapped by structural trapping (or the amount of the mobile supercritical phase CO_2) was very high during CO_2 injection (Fig. 7). In this scenario, the percentage of CO_2 trapped by structural trapping was about 21% at the end of the simulation period (980 years after the cessation of CO_2 injection).

The SFI for the scenario of the down-dip well with the lower section of middle sandstone layer (SS-2) injection was 0.79 at the storage time of 1000 years.

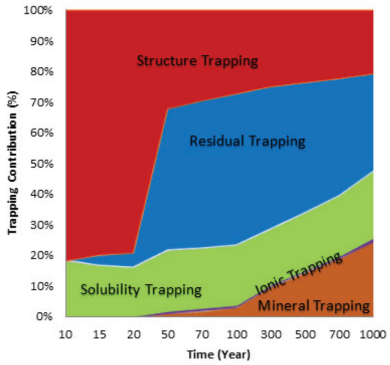

Fig. 7. Diagram of different trapping mechanisms' contributions for scenario (3)

5.4 Up-dip Well with the Lower Section of Middle Sandstone Layer (SS-2) Injection

For the scenario in which the injection well was located at the up-dip and CO_2 was injected into the lower section of the middle sandstone layer (SS-2), 88.98% of the injected CO_2 was stored by structural trapping, none by residual gas trapping, 10.38% by solubility trapping, 0.47% by ionic trapping, and 0.18% by mineral trapping at the end of the injection period (Table 5).

At the end of the simulation, the percentages of CO_2 trapped by the various trapping mechanisms were 70.91% by structural trapping, 7.36% by residual gas trapping, 8.73% by solubility trapping, 0.45% by ionic trapping, and 12.57% by mineral trapping (Table 5).

Table 5 Contributions of different trapping mechanisms changing with time for scenario (4)

Time (Year)	STM (%)	RTM (%)	SOTM (%)	ITM (%)	MTM (%)
1	69.08	1.55	29.26	0.12	0.00
10	84.07	0.00	15.60	0.31	0.03
15	88.34	0.00	11.11	0.44	0.12
20	88.98	0.00	10.38	0.47	0.18
50	80.71	7.57	10.16	0.57	1.00
70	79.94	8.08	9.91	0.55	1.52
100	79.23	8.45	9.56	0.53	2.24
300	77.15	8.50	8.17	0.43	5.77
500	75.12	8.46	7.89	0.41	8.12
700	73.38	8.08	8.07	0.42	10.05
1000	70.91	7.36	8.73	0.45	12.57

Abbreviations: See notes to Table 2.

There was no CO_2 trapped by residual gas trapping at the end of the injection period (20 years) because the well was located at the up-dip, which is unfavourable for the imbibition process. The percentage of CO_2 trapped by solubility trapping was also not very high during CO_2 injection (Fig. 8). The percentage of CO_2 trapped by mineral trapping was the second highest at the simulation time of 1000 years in the post-injection period (Fig. 8).

The percentage of CO_2 trapped by structural trapping was very high not only during CO_2 injection but also in the post-injection period (Fig. 8). It declined very slowly during the post-injection period because not much immobile residual CO_2 formed.

The SFI for the scenario of the up-dip well with the lower section of middle sandstone layer (SS-2) injection was 0.29 at the storage time of 1000 years.

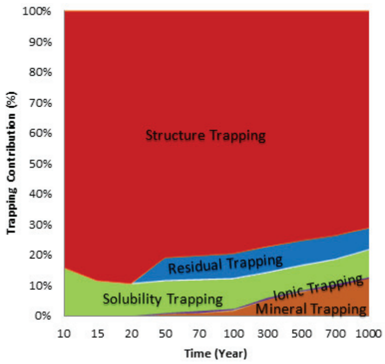

Fig. 8. Diagram of different trapping mechanisms' contributions for scenario (4)

5.5 Down-Dip Well with the Top Sandstone Layer (SS-1) Injection

For the scenario in which the injection well was located at the down-dip and CO_2 was injected into the top sandstone layer (SS-1), 79.88% of injected CO_2 was stored by structural trapping, 0.32% by residual gas trapping, 17.61% by solubility trapping, 0.65% by ionic trapping, and 1.55% by mineral trapping at the cessation of CO_2 injection (20 years) (Table 6).

At 980 years from the end of CO_2 injection, the percentages of CO_2 that were trapped by the different trapping mechanisms were 15.00% by structural trapping, 39.65% by residual gas trapping, 21.67% by solubility trapping, 1.09% by ionic trapping, and 22.58% by mineral trapping (Table 6).

Table 6 Contributions of different trapping mechanisms changing with time for scenario (5)

Time (Year)	STM (%)	RTM (%)	SOTM (%)	ITM (%)	MTM (%)
1	65.88	0.00	34.05	0.09	0.00
10	81.49	0.00	18.20	0.29	0.03
15	80.14	0.00	18.60	0.64	0.63
20	79.88	0.32	17.61	0.65	1.55
50	25.83	49.37	21.15	1.02	2.63
70	21.64	52.67	21.36	1.04	3.29
100	20.33	52.94	21.43	1.04	4.26
300	18.03	49.27	21.70	1.07	9.94
500	16.87	45.79	21.91	1.10	14.33
700	15.98	43.11	21.75	1.10	18.06
1000	15.00	39.65	21.67	1.09	22.58

Abbreviations: See notes to Table 2.

The percentage of CO_2 trapped by residual gas trapping was very low during CO_2 injection (Fig. 9). However, it was the highest during the post-injection period. The percentage of CO_2 trapped by solubility trapping was the second highest during CO_2 injection. The percentage of CO_2 trapped by mineral trapping was the second highest at the simulation time of 1000 years in the post-injection period (Fig. 9).

The percentage of CO_2 trapped by structural trapping was very high during CO_2 injection (Fig. 9). In this scenario, the percentage of CO_2 trapped by structural trapping was 15% at the end of the simulation period (980 years after the cessation of CO_2 injection).

The SFI for the scenario of the down-dip well with the top sandstone layer (SS-1) injection was 0.85 at the storage time of 1000 years.

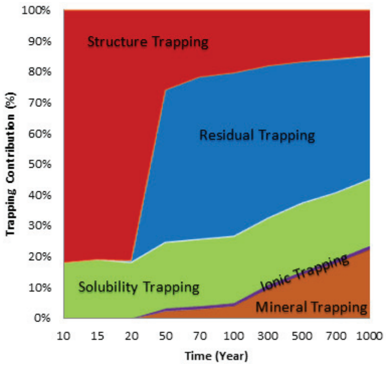

Fig. 9. Diagram of different trapping mechanisms' contributions for scenario (5)

5.6 Up-Dip Well with the Top Sandstone Layer (SS-1) Injection

For the scenario in which the injection well was located at the up-dip and CO_2 was injected into the top sandstone layer (SS-1), 88.08% of the injected CO_2 was trapped by structural trapping, none by residual gas trapping, 11.37% by solubility trapping, 0.40% by ionic trapping, and 0.15% by mineral trapping at the end of the injection period (Table 7).

At the end of the simulation, the percentages of CO_2 trapped by the various trapping mechanisms were 53.88% by structural trapping, 19.06% by residual gas trapping, 10.09% by solubility trapping, 0.49% by ionic trapping, and 16.45% by mineral trapping (Table 7).

Table 7 Contributions of different trapping mechanisms changing with time for scenario (6)

Time (Year)	STM (%)	RTM (%)	SOTM (%)	ITM (%)	MTM (%)
1	65.06	2.90	31.98	0.09	0.00
10	81.83	0.00	17.90	0.25	0.03
15	86.42	0.00	13.10	0.37	0.11
20	88.08	0.00	11.37	0.40	0.15
50	72.21	15.17	11.15	0.54	0.93
70	69.49	17.49	11.00	0.54	1.49
100	67.64	18.69	10.85	0.53	2.29
300	62.05	20.20	10.35	0.51	6.88
500	58.77	20.28	10.13	0.51	10.29
700	56.41	20.02	9.98	0.49	13.07
1000	53.88	19.06	10.09	0.49	16.45

Abbreviations: See notes to Table 2.

In this scenario, the percentage of CO_2 trapped by structural trapping (or the percentage of mobile supercritical phase CO_2) was very high during CO_2 injection (Fig. 10). There was no CO_2 trapped by residual gas trapping at the end of the injection period (20 years) because of the well location. The percentage of CO_2 trapped by solubility trapping was also not very high during CO_2 injection (Fig. 10). The percentage of CO_2 trapped by mineral trapping was not high at the simulation time of 1000 years in the post-injection period (Fig. 10).

The SFI for the scenario of the up-dip well with the top sandstone layer (SS-1) injection was 0.46 at the storage time of 1000 years.

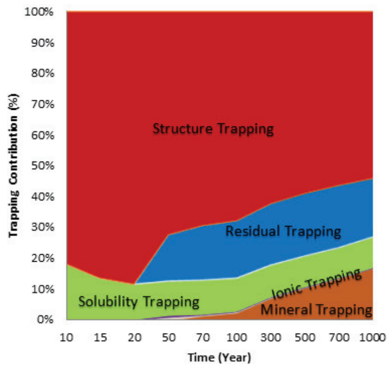

Fig. 10. Diagram of different trapping mechanisms' contributions for scenario (6)

6. Discussion

The risk of CO_2 leakage changes with time; therefore, the SFI is dynamic over the period of CO_2 storage. In this study, the SFI for evaluating the risk of leakage was calculated at various times for the scenarios of different well locations and different injection layers (Fig. 11).

The higher the SFI (i.e., the more moles of CO_2 trapped by the safe trapping mechanisms), the safer the CO_2 sequestration. During CO_2 injection, the amount of CO_2 trapped by structural trapping was very high and led to a low SFI (Fig. 11). In the post-injection period, the safe trapping mechanisms contributed to a lower risk of CO_2 leakage by trapping CO_2 as immobile blobs or changing the phase of CO_2 from supercritical phase to aqueous, ionic, and mineral phases.

In this case study of complex sandstone-shale sequences in an aquifer, the SFI for the case of injecting CO_2 into the bottom sandstone layer (SS-3) was higher than that of the others (SS-1 or SS-2). The second shale layer (SH-2) overlaid on the bottom sandstone layer (SS-3) helped the CO_2 plume migrate farther into the SS-3 layer; consequently, the residual CO_2 (immobile supercritical phase CO_2) was rapidly and widely formed in the early post-injection period. The middle sandstone layer (SS-2) had better transmissibility for CO_2 injectivity, but it was not the best solution for storage safety based on the results of risk evaluation and the SFI estimation.

Residual gas trapping had the greatest influence on storage safety in the early post-injection period. One of the best engineering techniques for safety-based injection strategy is to maximize the amount of trapped CO_2 by residual gas trapping in order to lower the risk of CO_2 leakage in subsequent decades.

The well location is a critical factor that affects a safety-based injection strategy. The risk of CO_2 leakage is lower when using a down-dip injection well than an up-dip well (Fig. 11). In the scenarios of CO_2 injected into the top sandstone (SS-1), the SFI for the down-dip well was twice that for the up-dip well at the storage time of 1000 years.

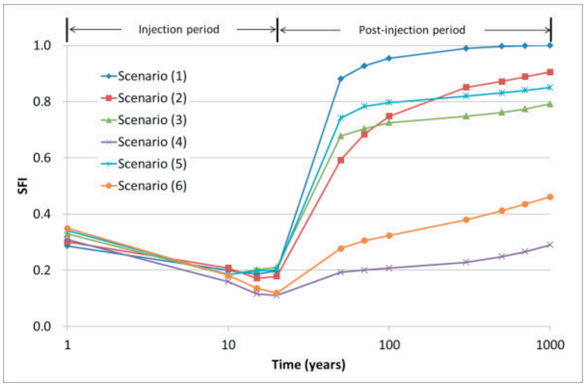

Fig. 11. Estimation of the safety index's changing with time for six scenarios

The best engineering strategy for this case study was to inject CO_2 from the down-dip well with a perforation in the interval of the bottom sandstone layer (i.e., scenario (1)), based on the estimation of the SFI. The SFI for this scenario reached 0.99 at the storage time of 1000 years, which meant that the probability of a CO_2 leak occurring was nearly zero.

7. Conclusions

The conclusions obtained in this study are:

(1) The risk of CO_2 leakage changed with time. It can be estimated using the safety index (SFI). During CO_2 injection, the amount of CO_2 trapped by structural trapping was very high and led to a low SFI. In the post-injection period, the safe trapping mechanisms contributed to a lower risk of CO_2 leakage by trapping CO_2 as immobile blobs or changing the phase of CO_2 from supercritical phase to aqueous, ionic, and mineral phases.

(2) In this case study of complex sandstone-shale sequences in an aquifer, the SFI for the scenario of injecting CO_2 into the bottom sandstone layer (SS-3) was higher than that of the others (SS-1 or SS-2). The middle sandstone layer (SS-2) had better transmissibility for CO_2 injectivity but was not the best solution for storage safety, based on the results of risk evaluation and the estimated SFI.

(3) The well location is a critical factor that affects a safety-based injection strategy. The risk of CO_2 leakage is lower when using a down-dip injection well than an up-dip well.

(4) The best engineering strategy for this case study was to inject CO_2 into a down-dip well with a perforation in the interval of the bottom sandstone layer. The SFI for this scenario reached 0.99 at the storage time of 1000 years, which meant that the probability of a CO_2 leak occurring was nearly zero.

Acknowledgments

This study was supported by grant NSC 101-3113-E-008-002 from the Taiwan National Science Council, National Science and Technology Program-Energy (NSTP-Energy).

References

[1] IPCC. Special Report on Carbon Dioxide Capture and Storage. Metz, B., Davidson, O., de Coninck, H., Loos, M., Meyer, L.A. (Eds.). New York: Cambridge University Press; 2005.

[2] IEA. CO2 Capture and Storage—A Key carbon abatement option. 2008.

[3] Shukla R, Ranjith P, Haque A, Choi X. A review of studies on CO2 sequestration and caprock integrity. Fuel 2010;89:2651-2664.

[4] Thibeau S, Nghiem L, Ohkuma H. A Modeling Study of the Role of Selected Minerals in Enhancing CO2 Mineralization During CO2 Aquifer Storage. Paper SPE 109739 presented at the 2007 SPE Annual Technical Conference and Exhibition. Anaheim, California 2007.

[5] Shen CH, Hsieh BZ, Tseng CC, Lin ZS. Case Study of CO2 Sequestration Affected by Different Trapping Mechanisms. Paper presented at the 2011 Asia Oceania Geosciences Society (AOGS). Taipei 2011.

[6] CMG. User's Guide GEM Advanced Oil/Gas Reservoir Simulator. Calgary: Computer Modelling Group Ltd.; 2011.

[7] Kumar A, Noh MH, Sepehrnoori K, Pope GA, Bryant SL, Lake LW. Simulating CO2 storage in deep saline aquifers. In: Carbon Dioxide Capture for Storage in Deep Geologic Formations—Results from the CO2 Capture Project, Vol. 2: Geologic Storage of Carbon Dioxide with Monitoring and Verification. London: Elsevier; 2005, p. 898-977.

[8] Nghiem L, Sammon P, Grabenstetter J, Ohkuma H. Modeling CO2 Storage in Aquifers with a Fully-Coupled Geochemical EOS Compositional Simulator. Paper SPE 89474 presented at the 2004 SPE/DOE Symposium on Improved Oil Recovery. Tulsa, Oklahoma 2004.

[9] Nghiem L, Tran D, Hassam M, Yang D. Simulation of CO2 Storage in Saline Aquifers. Paper SPE 125848 presented at the 2009 SPE/EAGE Reservoir Characterization and Simulation Conference. Abu Dhabi 2009.